Datum Effects on the Stability of the Celestial Reference Frame Determined by VLBI

Virginia Raposo-Pulido[1,2], Robert Heinkelmann[2], Julian A. Mora-Diaz[2], Minghui Xu[2], Tobias Nilsson[2], Maria Karbon[2], Li Liu[2], Cuixian Lu[2], Benedikt Soja[2], Harald Schuh[2]

Abstract In this work, we investigate the small differences in realizations of the Celestial Reference Frame (CRF) by applying different celestial datum definitions to our new GFZ VLBI solution. The approaches are based on the geometric distribution, the astrophysical quality, and the number of radio sources. The effects on the axes stability of the frame are assessed by several statistical measures. The results show how the differences among the rotation angles are more sensitive to the astrophysical quality than to the number of radio sources chosen to define the datum. The global rotations show values up to 21 μas when comparing datums with different numbers of radio sources and up to 45 μas when comparing datums with different astrophysical quality, where radio sources with declinations below $-50°$ are not found. Besides, the regions where more radio sources need to be observed (generally below $-50°$ in declination) are plotted in the conclusions.

Keywords celestial datum, Vienna VLBI Software (VieVS), Celestial Reference Frame (CRF)

1 Introduction

When estimating a CRF in VLBI analysis, usually a number of radio sources with a long history of observations and stable positions are used to determine the orientation of the estimated frame w.r.t. the previous frame. Thereafter an additional small set of rotations relates the frame to the initial orientation as given by the International Celestial Reference System (ICRS). For the second realization of the International Celestial Reference Frame (ICRF2), 295 radio sources called "defining sources" were chosen to define the orientation of the axes, following the criteria specified by the IERS Technical Note 35 (Fey et al., 2009). For the improvement of the axes definition, the ICRF2 defining sources were chosen not only depending on their astrometric and astrophysical qualities, but also depending on their geometrical distribution, particularly in the south. Consequently, some radio sources were possibly included in spite of being variable in both flux and structure. Positions of those radio sources could become significantly variable with time, which would degrade the accuracy of the datum.

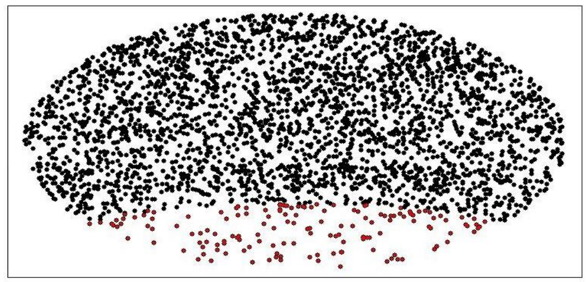

Fig. 1 Radio sources included in the GFZ global VLBI solutions. 151 radio sources have declinations below $-40°$.

2 Data and Methods

In order to assess the celestial datum effects, global VLBI solutions were calculated with the new GFZ VLBI solution (Heinkelmann et al., 2014). 3,341

1. IGN, National Geographic Institute, Madrid, Spain
2. Helmholtz Centre Potsdam, GFZ German Research Centre for Geosciences

sessions were analyzed with the GFZ version of the Vienna VLBI Software (VieVS, Böhm et al., 2012), applying the IERS Conventions (Petit and Luzum, 2010). In this work, we only use sessions that are from the period 1990-2013 and have more than three stations. The sessions were selected taking into account the small number of radio sources with good astrophysical quality before 1990 and the limitations of the VLBI networks at that time. The terrestrial datum was realized by applying no-net-translation (NNT) and no-net-rotation (NNR) conditions for all stations except those affected by earthquakes and the recently built ones, which are not included in the International Terrestrial Reference Frame 2008 (ITRF2008, Altamimi et al., 2011). With this criterion, the stations left out of the datum were: TSUKUB32, KOGANEI, KASHIM11, KASHIM34, TIGOCONC, SINTOTU3, VERAMZSW, YARRA12M, WARK12M, and KATH12M. Furthermore, 14 additional stations were found with not enough data to estimate reliable velocities, most of them being mobile occupation or radio astronomy telescopes. Therefore, they were reduced session-wise in the analysis. The global solutions considered only radio sources with more than two observations (see Figure 1), excluding the remaining sources to avoid singularity problems. The 39 special handling sources were reduced session-wise due to their time-dependent large structures.

The axes stability was assessed by estimating the angles of a 3D rotation (A_1, A_2, and A_3) and two shearing or deformation parameters (D_α and D_δ):

$$d\alpha = A_1 tan\delta_1 cos\alpha_1 + A_2 tan\delta_1 sin\alpha_1 - A_3 + D_\alpha \delta_1$$

$$d\delta = -A_1 sin\alpha_1 + A_2 cos\alpha_1 + D_\delta \delta_1$$

where (α_1, δ_1) are the a priori source coordinates taken from the ICRF2 and ($d\alpha$, $d\delta$) the differences of coordinates in the two frames.

3 Analysis Based on the Number of Radio Sources

The concept used in this analysis was to divide the celestial sphere into an equally spaced 20° by 20° grid, i.e., 18×9 fields. The effects due to the number of radio sources, the density, were assessed by keeping the geometrical distribution constant. For the datum definition, NNR conditions were applied for five levels of densification (see Figs. 2–6): A (156 radio sources), B

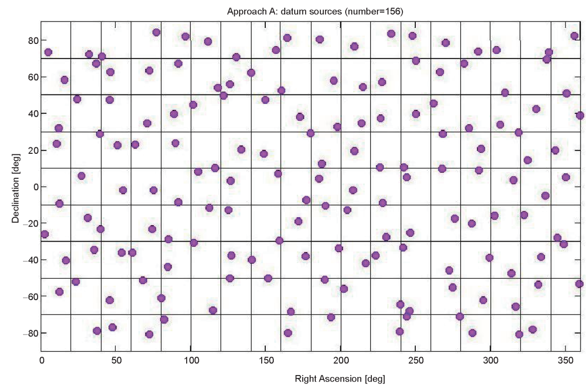

Fig. 2 Radio sources included in the datum for approach A (156 sources).

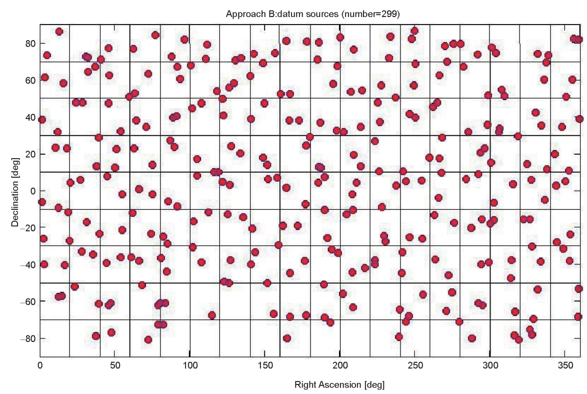

Fig. 3 Radio sources included in the datum for approach B (299 sources).

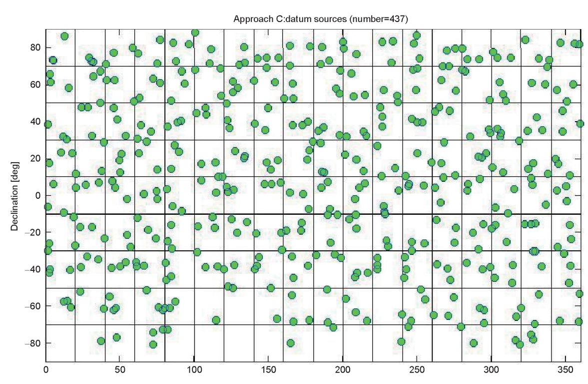

Fig. 4 Radio sources included in the datum for approach C (437 sources).

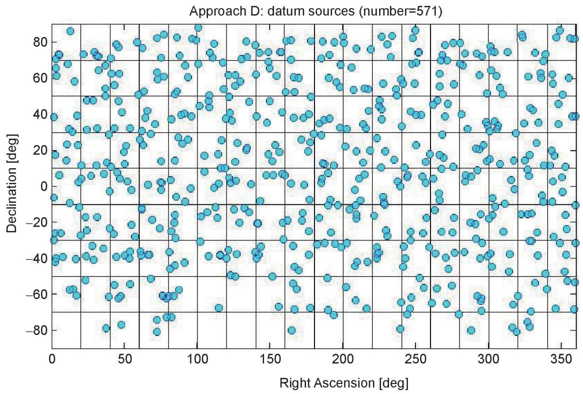

Fig. 5 Radio sources included in the datum for approach D (571 sources).

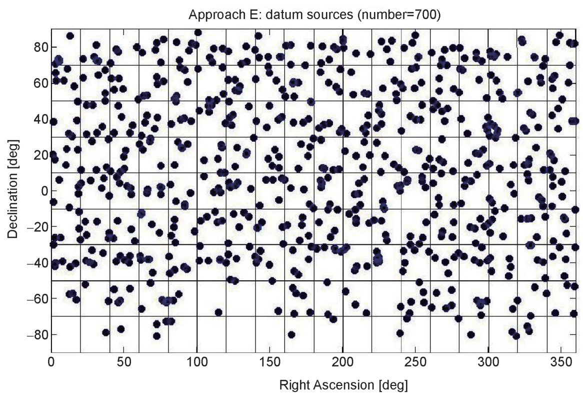

Fig. 6 Radio sources included in the datum for approach E (700 sources).

(299 radio sources), C (437 radio sources), D (571 radio sources), and E (700 radio sources).

Table 1 Transformation parameters w.r.t. ICRF2 using different approaches (A, B, C, D, and E).

	A_1 [μas]	A_2 [μas]	A_3 [μas]	D_α [μas/deg]	D_δ [μas/deg]
A	10.8 ± 6.0	17.5 ± 6.9	9.1 ± 7.7	0.3 ± 0.2	0.2 ± 0.1
B	13.0 ± 4.7	17.1 ± 5.3	2.6 ± 5.7	0.1 ± 0.2	0.1 ± 0.1
C	16.7 ± 5.1	15.9 ± 5.8	1.2 ± 6.1	0.1 ± 0.2	0.1 ± 0.1
D	17.8 ± 5.3	13.9 ± 5.9	2.2 ± 6.1	0.2 ± 0.2	0.2 ± 0.1
E	20.2 ± 5.1	14.5 ± 5.8	0.5 ± 5.9	0.2 ± 0.2	0.2 ± 0.1

The orientation parameters (see Table 1) show variations between the different approaches smaller than 10 μas, the current level of axes stability specified for ICRF2. However, A_1 and A_2 frame rotations are all positive between about 10 to 20 μas for all the investigated densifications. This is due to the comparison of different selected data (1979–2009 for ICRF2 vs. 1990–2013 in this work). The formal errors are between about 5 and 6 μas. The rotation around the z-axis A_3 shows differences among the approaches that are relatively larger, but of less significance. The values are smaller than 21 μas but indicate a systematic rotation w.r.t. ICRF2. The deformation parameters w.r.t. ICRF2 are negligible and almost insignificant.

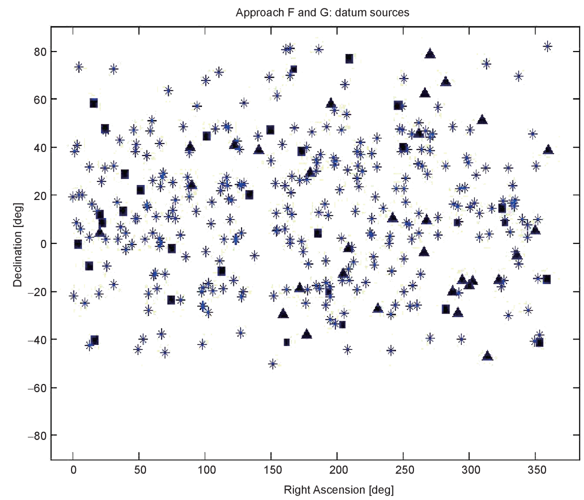

Fig. 7 Datum sources for approaches F and G: 296 radio sources in common (asterisk), 31 sources for approach G with an S-band SI larger than 2 (triangle), and 31 sources different from the approach G sources for approach F (square).

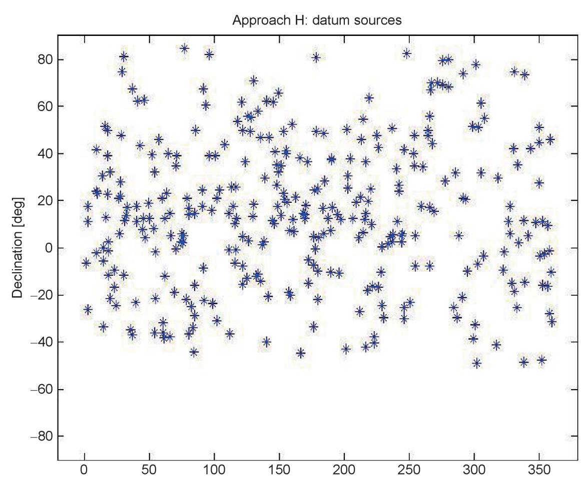

Fig. 8 Datum sources for approach H: 327 radio sources different from approaches F and G.

4 Analysis Based on the Astrophysical Quality

The concept used in this analysis was to choose sets of radio sources with different structure indices (SI, Fey et al., 1997). The effects due to astrophysical quality were assessed by keeping the number of radio sources constant. For the datum definition, three sets of datum sources were investigated: F, G, and H. Set F includes only those radio sources with X-band SI and S-band SI smaller than three, G considers only radio sources with an X-band SI smaller than three (see Figure 7), and H considers radio sources with an X-band SI greater than two (see Figure 8). Datum subsets F to H all contain 327 radio sources in total, which was the maximum number of radio sources with X-band and S-band SI smaller than three in the GFZ global solution. A total of 358 radio sources were found with X-band SI smaller than three (31 out of 358 with S-band SI larger than two) and 370 with X-band SI larger than two. For that reason, 296 radio sources in common between the approaches F and G were selected, and 31 alternate sources (around 10% of the total number) were selected. Approach H does not contain any radio source in common with F and G.

Table 2 Transformation parameters w.r.t. ICRF2 using different approaches F, G, and H.

	A_1 [μas]	A_2 [μas]	A_3 [μas]	D_α [μas/deg]	D_δ [μas/deg]
F	14.2 ± 6.0	44.5 ± 6.8	-24.7 ± 6.7	0.3 ± 0.2	0.0 ± 0.1
G	14.2 ± 6.3	39.5 ± 7.2	-19.3 ± 6.9	0.2 ± 0.2	0.0 ± 0.1
H	16.8 ± 7.1	-8.0 ± 7.7	-10.6 ± 7.6	0.0 ± 0.2	0.2 ± 0.1

The orientation parameters (see Table 2) reach significant values up to 45 μas. This results in significant frame rotations, which are partly due to the comparison of data based on different periods (1979-2009 vs. 1990-2013) and the deficient geometry considered by this approach. The three sets of datum sources do not contain radio sources below about $-50°$ in declination. Consequently, the transformation parameters should only be interpreted relatively w.r.t. each other. In that case, the orientation parameters (see Table 2) show variations between approaches F and G smaller than 6 μas and up to 53 μas when approach H is considered in the comparison. The formal errors are between about 6 and 7 μas, being the largest for approach H. The deformation parameters w.r.t. ICRF2 are negligible and almost insignificant.

5 Conclusions

The current number of defining sources is 295. The first analysis shows that this number can be increased with no significant detriment to the frame. The second analysis deals with approaches F, G, and H with approximately the same geometry but different radio sources depending on the SI. The relative rotation angles are larger for the second analysis than for the first analysis. The differences are more significant when the astrophysical quality is considered instead of the number of radio sources.

The X-band and S-band SI information was available for 728 and 701 out of 3,254 radio sources, respectively (www.obs.u-bordeaux1.fr/BVID/). The plots of the second analysis show the lack of radio sources with small SI or SI information for declinations below $-50°$. It means that more observations for imaging are necessary in the south to cover that declination range. Regions have been found for declinations below $-45°$ (see Figure 9) with no radio sources (for extreme right ascensions) or just one source. More observations in these regions should be done to have a uniform distribution over the sky.

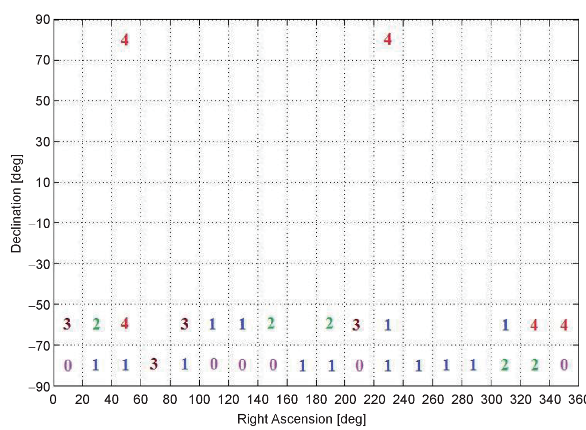

Fig. 9 Grids, where the radio sources are missing (0 radio sources) or no radio sources could be added for densification (1, 2, 3, or 4 radio sources) for the first analysis. The empty grids contain more than 4 radio sources.

Acknowledgements

We acknowledge IGN for its support and IVS for providing the data analyzed in this study.

References

1. Z. Altamimi, X. Collilieux, and L. Métivier (2008). ITRF2008: an improved solution of the international terrestrial reference frame. *Journal of Geodesy, Volume 85, Issue 8, pp. 457–473*. doi: 10.1007/s00190-011-0444-4.
2. J. Böhm, S. Böhm, T. Nilsson, A. Pany, L. Plank, H. Spicakova, K. Teke, and H. Schuh (2012). The New Vienna VLBI Software VieVS. *S. Kenyon et al. (eds.), Geodesy for Planet Earth, International Association of Geodesy Symposia 136. Springer-Verlag Berlin Heidelberg, 2012*. doi: 10.1007/978-3-642-20338-1_126.
3. A. L. Fey and P. Charlot (1997). VLBA Observations of radio reference frame sources. III: Astrometric suitability of an additional 225 sources. *The Astrophysical Journal Supplement Series, 128, pp. 17–83*.
4. A. L. Fey, D. Gordon, and C. S. Jacobs (eds.) (2009). The Second Realization of the International Celestial Reference Frame by Very Long Baseline Interferometry. *Presented on behalf of the IERS / IVS Working Group (IERS Technical Note No. 35). Frankfurt am Main: Verlag des Bundesamts für Kartographie und Geodäsie, p.204*. ISBN 3-89888-918-6.
5. R. Heinkelmann, T. Nilsson, M. Karbon, L. Liu, C. Lu, J. Mora-Diaz, E. Parselia, V. Raposo-Pulido, B. Soja, M. Xu, and H. Schuh (2014). The GFZ VLBI Solution — Characteristics and First Results. *IVS General Meeting 2014 Proceedings*, this volume.
6. G. Petit and B. Luzum (2010). IERS Conventions (2010). *(IERS Technical Note No. 36) Frankfurt am Main: Verlag des Bundesamts für Kartographie und Geodäsie, p. 179*. ISBN 3-89888-989-6.